Supplementary material to the manuscript

Brief Communication: Ice older than a century at Triglav Glacier and Skuta Glacier – isotopic characteristics of glacier remains in Southeastern Alps, Slovenia

László Palcsu[1*], Marjan Temovski[1,2*], Danny Vargas[1], Matteo Nigro[3], Christoph Henrich[4,a] Yuliya Vystavna[5], Matija Zorn[6], Matej Lipar[6], Miha Pavšek[6], Jure Tičar[6], Klara Žagar[7], Polona Vreča[7]

[1]Isotope Climatology and Environmental Research Group, HUN-REN Institute for Nuclear Research (ATOMKI), Debrecen, Hungary
[2]Department of Mineralogy and Geology, University of Debrecen, Debrecen, Hungary
[3]Department of Agriculture, Food, Environment and Forestry, University of Florence, Firenze, Italy
[4]Department of Technical Cooperation, International Atomic Energy Agency, Vienna, Austria
[5]Isotope Hydrology Section, International Atomic Energy Agency, Vienna International Centre, Vienna, Austria
[6]Anton Melik Geographical Institute, Research Centre of the Slovenian Academy of Sciences and Arts, Ljubljana, Slovenia
[7]Department of Environmental Sciences, Jožef Stefan Institute, Ljubljana, Slovenia,

* Correspondence: László Palcsu (palcsu.laszlo@atomki.hu), Marjan Temovski (temovski.marjan@atomki.hu)

Ground penetrating radar survey

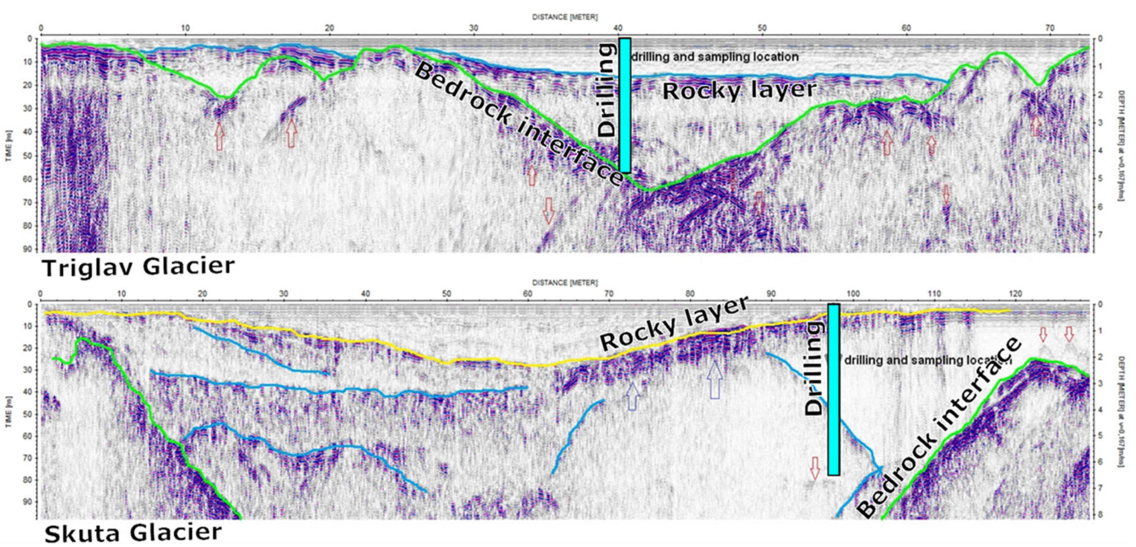

Figure S1. Georadar profiles of the Triglav Glacier and the Skuta Glacier. The grey arrows represent the drilling location and depth. The blue and yellow lines represent contrasts in the ice volume. The green lines identify the ice to bedrock transition (Nigro et al., 2026).

[a] present address: The University of the South Pacific, Centre for Sustainable Futures, Laucala Campus, Suva, Fiji.

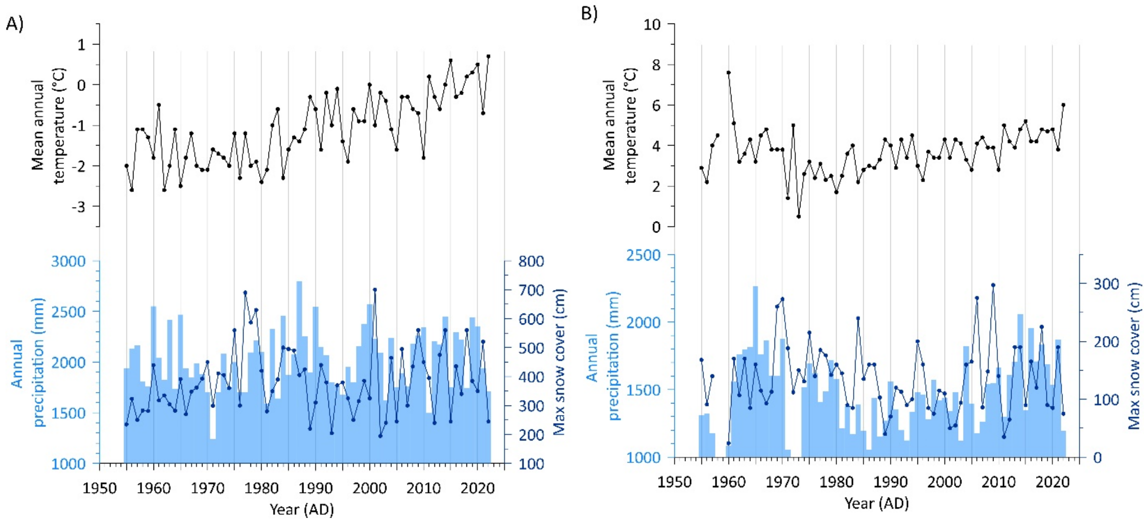

Figure S2. Meteorological data at Mt. Kredarica (2,513 m; Julian Alps) (A) and Mt. Krvavec (1,748 m; Kamnik-Savinja Alps) (B) meteorological stations.

Sampling

Figure S3. Sampling approach at Triglav Glacier (A-C) and Skuta Glacier (D-E). A – Start of ice coring from the snow-covered ice mass at Triglav Glacier. B – Laterally dug trench to bypass the rocky layer at 0.9-1.0 m. Note that the stratigraphy of the trench, with top 10 cm represented by snow, bracketed by dust layers on top and below it, followed by firn ice down to a depth of ~70 cm, and ice further down, with a rocky layer at depth of 0.9-1.0 m. C – Subsampling by cutting the ice core in 10 cm-long sections. Note the open topography around Triglav Glacier.

D – The closed cirque hosting Skuta Glacier. E – Start of ice coring at Skuta Glacier. Note the dust and rock fragments covering the ice surface. F – Subsampling by cutting the ice core in 10 cm-long sections.

Sampling

The sampling locations for ice cores drilling at Triglav Glacier and Skuta Glacier were selected based on the field inspection and GPR data obtained in 2022 prior to our survey (Supplementary Figure S1). Drilling at both glaciers was performed with a hand auger (Mark II, Kovacs Ice Drilling and Coring Equipment) in late August 2022 (Supplementary Figure S2). Four cores were extracted at Triglav Glacier (Table S1). Drilling was started at ~10 cm depth, marked by a dark layer at the boundary between snow and firn (depth datum 0.00 m). A 0.94 m long core (A) was retrieved, with drilling further prevented by a rocky layer. Similarly, the rocky layer was reached next to it, retrieving a 0.72 m long core (B). To bypass the rocky layer, a trench was dug laterally towards the drilled core position, down to the depth of ~1 m (Supplementary Figure S2 and Table S1). Sample was collected from the ice in the rocky layer at depth 0.90-1.00 m (R0.9). Plant stems were found in the upper part of the rocky layer, of which a sample was taken for ^{14}C analysis. Two cores were drilled below the rocky layer, a 2.72 m long core (C) and a 3.10 m long core (D). The top 10 cm snow above cores A and B (depth -0.10 to 0.00 m) was collected as samples A-T and B-T, respectively. The maximum drilling depth reached at Triglav Glacier was 4.5 m taken from the surface (or 4.4 m if taken from datum 0.00).

At Skuta Glacier, in addition to the GPR measurements, two test cores were drilled to probe for possible rocky layers, intercepting them at depth of ~4 m (surface taken as datum, 0.00 m). Following that, a 0.70 m long ice core (E) was retrieved, with drilling further prevented by a rocky layer. Next to it, ice core (F) was retrieved down to the depth of 6.43 m, where also a rocky layer was intercepted. No macrofossils were observed therefore no sample was collected for ^{14}C analysis at Skuta Glacier.

The retrieved ice cores were cut into 10 cm long sections to collect 80 and 72 samples for further analysis from Triglav and Skuta ice masses, respectively. Samples were double packed in Whirl-Pak Standard sampling bags and let melt at room temperature. Subsamples of the melted ice samples were separated for the laboratories of the Jožef Stefan Institute in Ljubljana, Slovenia (JSI) and HUN-REN Institute for Nuclear Research in Debrecen, Hungary (ATOMKI). Subsamples for δ^2H and $\delta^{18}O$ analysis were collected in 30 mL HDPE bottles. For radioisotope analysis (^3H, ^7Be, ^{137}Cs and ^{210}Pb), subsamples from selected ice core sections were combined in a composite as presented in Supplementary Table S2.

Table S1. Summary of collected cores and samples at Triglav and Skuta glaciers

Core	Core length (m)	Maximum depth from 0.00 datum (m)	Number of collected samples	Comment
TRIGLAV GLACIER				
A	0.94	0.94	10	Datum 0.00 is taken as the boundary between snow and firn at ca. 10 cm from surface
B	0.72	0.72	8	As for core A
C	2.72	3.72	28	Starting at 1 m depth, below the rocky layer
D	3.10	4.40	31	Starting at 1.3 m depth, below the rocky layer
R	0.10	1.00	1	Sample from the rocky layer between 0.9 and 1 m depth
A-T	0.10	-0.10	1	Snow above 0 datum at core A
B-T	0.10	-0.10	1	Snow above 0 datum at core B

SKUTA GLACIER				
E	0.7	0.7	7	Datum 0.00 is taken at the surface
F	6.43	6.43	65	

Stable isotope analysis

Isotopic composition of hydrogen (δ^2H) and oxygen (δ^{18}O) was determined in all 152 collected ice core samples at JSI on a dual inlet isotope ratio mass spectrometer (Finnigan MAT DELTA plus, Finnigan MAT GmbH, Bremen, Germany) with an automated H_2-H_2O and CO_2-H_2O equilibrator. Samples (3 mL) were measured in duplicates and allowed to equilibrate for two (H_2-H_2O) and six (CO_2-H_2O) hours before analysis (Vreča et al., 2024, Lancaster et al., 2025; Nigro et al., 2026). All measurements were conducted in conjunction with laboratory reference materials calibrated periodically against primary IAEA calibration standards to the VSMOW/SLAP scale. The results were normalized to VSMOW/SLAP using two-point normalization in LIMS (Laboratory Information Management System for Light Stable Isotopes) program and are expressed in the conventional delta (δ) notation (in ‰). The average sample repeatability was 0.2 ‰ for δ^2H and 0.02 ‰ for δ^{18}O. Deuterium excess (d-excess) was calculated as d-excess = δ^2H − 8 x δ^{18}O. Duplicate samples for water stable isotopes were analyzed also at HUN-REN Institute for Nuclear Research (ATOMKI), Debrecen, Hungary, for intercomparison (Nigro et al., 2026).

Radioisotope analysis

For analysis of tritium concentration (^{3}H) in 31 merged ice core samples (Supplementary Table S2), the ^{3}He-ingrowth method was used. The melted ice samples were poured into stainless steel vessels equipped with all-metal valves. The headspace and the dissolved gases were completely removed by vacuum pumping. After degassing, the samples were stored for ^{3}He production from tritium decay for a few weeks. The absolute amount of tritiogenic helium was then determined by a Helix SFT helium mass spectrometer at ATOMKI. To increase the accuracy, a well-known aliquot of a pure ^{4}He spike was added to each sample during before the mass spectrometric measurement (Palcsu et al., 2010). The measurement was calibrated with well-known air aliquots (Papp et al., 2012). The tritium concentration is expressed in tritium units (TU), where 1 TU represents a ^{3}H/^{1}H isotope ratio of 10^{-18}. In case of water, 1 TU equals to 0.119 Bq/kg activity concentration. The detection limit is lower than 0.02 TU, while the uncertainty is better than 2 % above 1 TU.
Caesium-137, beryllium-7 as well as lead-210 were analyzed in 20 combined ice core samples with gamma-spectrometry at ATOMKI. Since, caesium, beryllium and lead are suspected to be adsorbed in solid particles, the ice samples were filtered with cellulose-acetate membrane filters of 0.45 µm mesh size. Using the filters, the activity of ^{7}Be, ^{137}Cs and ^{210}Pb is then determined with a high-purity germanium detector (Canberra-Packard BE50307915-30ULB thin-windowed planar HPGe detector, 35% relative efficiency) (Janovics et al., 2014).
The radiocarbon (^{14}C) content of the plant stem collected in the rocky layer at Triglav Glacier was analyzed by accelerator mass spectrometry (AMS) (Molnár et al., 2013) at ATOMKI. The AMS measurement of the samples was normalized to the NIST oxalic acid (oxalic acid standard, SRM-4990C), and expressed as Fraction Modern ($F^{14}C$). The final calibrated radiocarbon age was determined using the CALIBomb calibration (http://calib.org).

Data evaluation

For construction of the age-depth models, Triglav Glacier and Skuta Glacier δ^{18}O time series composite records were created by averaging the values of the different extracted cores according to their depth. The records were tuned using tie-points radiometrically and visually defined using the lake Jezero v Ledvicah (1,830 m; located ~6 km southwest from Triglav

Glacier; Dobravec and Šiško, 2002) annual air-temperature reconstruction (Battarbee et al., 2002). Tie-points were determined and assigned using the QAnalySeries software (Kotov and Paelike, 2018) using each ice-core record as an input and the Jezero v Ledvicah as target.
The spectral analysis of Triglav Glacier and Skuta Glacier δ^{18}O records as function of depth was carried out using the Continous Wavelet Transform (Grinsted et al., 2004) available in the Acycle v2.8 MATLAB package (Li et al., 2019) described in Supplementary Figure S4. The significant band periods were determined using an AR(1) noise surrogate that captures the short-memory processes in the records. The annual temperature (°C) was extracted from the Climate Research Unit (CRU) TS Version 4.08 gridded datasets at a spatial resolution of 0.5° latitude by 0.5° longitude (Harris et al., 2020).

Isotope Data

Table S2. Stable isotope results for Triglav Glacier and Skuta Glacier.

Core	Sample	Depth (cm)			Lab code	δ^{18}O	±	δ^{2}H	±	d-excess
		from	to	mid		‰ VSMOW				
TRIGLAV										
A	A-T	-10	0	-5	I22-750	-8.15	0.02	-53.0	0.1	12.2
	A0.0	0	10	5	I22-751	-7.06	0.02	-44.7	0.1	11.8
	A0.1	10	20	15	I22-752	-7.07	0.00	-45.3	0.0	11.3
	A0.2	20	30	25	I22-753	-7.18	0.04	-46.5	0.2	10.9
	A0.3	30	40	35	I22-754	-7.26	0.03	-46.9	0.2	11.2
	A0.4	40	50	45	I22-755	-7.25	0.05	-47.0	0.4	11.0
	A0.5	50	60	55	I22-756	-7.32	0.03	-47.1	0.0	11.5
	A0.6	60	70	65	I22-757	-7.46	0.04	-47.9	0.5	11.8
	A0.7	70	80	75	I22-758	-7.95	0.01	-51.9	0.4	11.7
	A0.8	80	90	85	I22-759	-9.62	0.00	-63.6	0.3	13.4
	A0.9	90	100	95	I22-760	-9.77	0.01	-65.6	0.0	12.6
B	B-T	-10	0	-5	I22-761	-8.12	0.03	-53.3	0.7	11.7
	B0.0	0	10	5	I22-762	-7.56	0.02	-49.4	0.3	11.1
	B0.1	10	20	15	I22-763	-7.59	0.00	-50.1	0.0	10.6
	B0.2	20	30	25	I22-764	-7.59	0.01	-49.8	0.4	10.9
	B0.3	30	40	35	I22-765	-7.67	0.02	-50.3	0.3	11.1
	B0.4	40	50	45	I22-766	-7.76	0.01	-50.9	0.1	11.2
	B0.5	50	60	55	I22-767	-7.81	0.02	-50.7	0.2	11.8
	B0.6	60	70	65	I22-768	-7.99	0.02	-52.2	0.0	11.7
	B0.7	70	80	75	I22-769	-8.29	0.02	-54.0	0.0	12.3
C	C1.0	100	110	105	I22-770	-8.59	0.00	-55.2	0.0	13.5
	C1.1	110	120	115	I22-771	-8.67	0.06	-55.6	0.4	13.8
	C1.2	120	130	125	I22-772	-8.66	0.05	-55.2	0.4	14.1
	C1.3	130	140	135	I22-773	-8.62	0.03	-55.4	0.3	13.6
	C1.4	140	150	145	I22-774	-8.59	0.03	-55.4	0.1	13.3
	C1.5	150	160	155	I22-775	-8.47	0.02	-54.1	0.0	13.7
	C1.6	160	170	165	I22-776	-8.50	0.02	-53.9	0.3	14.1
	C1.7	170	180	175	I22-777	-8.55	0.01	-54.7	0.1	13.7
	C1.8	180	190	185	I22-778	-8.39	0.03	-54.1	0.6	13.0
	C1.9	190	200	195	I22-779	-8.68	0.01	-55.0	0.4	14.4
	C2.0	200	210	205	I22-780	-9.32	0.01	-60.6	0.5	14.0

	C2.1	210	220	215	I22-781	-9.29	0.00	-60.7	0.3	13.6
	C2.2	220	230	225	I22-782	-9.34	0.00	-60.4	0.2	14.3
	C2.3	230	240	235	I22-783	-9.03	0.02	-59.2	0.1	13.0
	C2.4	240	250	245	I22-784	-8.81	0.03	-57.4	0.5	13.1
	C2.5	250	260	255	I22-785	-8.84	0.01	-56.7	0.5	14.0
	C2.6	260	270	265	I22-786	-8.96	0.01	-57.7	0.3	14.0
	C2.7	270	280	275	I22-787	-8.64	0.01	-55.5	0.2	13.6
	C2.8	280	290	285	I22-788	-8.50	0.02	-54.5	0.1	13.5
	C2.9	290	300	295	I22-789	-8.61	0.01	-55.8	0.2	13.1
	C3.0	300	310	305	I22-790	-9.11	0.02	-59.4	0.2	13.5
	C3.1	310	320	315	I22-791	-9.07	0.02	-59.4	0.5	13.2
	C3.2	320	330	325	I22-792	-8.66	0.01	-56.3	0.1	13.0
	C3.3	330	340	335	I22-793	-8.83	0.03	-57.4	0.1	13.2
	C3.4	340	350	345	I22-794	-8.26	0.01	-52.7	0.3	13.4
	C3.5	350	360	355	I22-795	-8.19	0.01	-53.1	0.3	12.4
	C3.6	360	370	365	I22-796	-8.39	0.01	-54.3	0.2	12.8
	C3.7	370	380	375	I22-797	-8.33	0.01	-53.7	0.1	12.9
D	D1.3	130	140	135	I22-798	-8.56	0.00	-55.6	0.1	12.9
	D1.4	140	150	145	I22-799	-8.44	0.01	-54.6	0.2	12.9
	D1.5	150	160	155	I22-800	-8.39	0.01	-53.8	0.1	13.3
	D1.6	160	170	165	I22-801	-8.52	0.03	-53.9	0.1	14.3
	D1.7	170	180	175	I22-802	-8.42	0.04	-53.7	0.0	13.7
	D1.8	180	190	185	I22-803	-8.50	0.02	-54.0	0.0	14.0
	D1.9	190	200	195	I22-804	-8.85	0.00	-57.1	0.2	13.7
	D2.0B	200	210	205	I22-806	-9.23	0.01	-59.7	0.0	14.1
	D2.1	210	220	215	I22-807	-9.22	0.00	-59.4	0.4	14.4
	D2.0A	220	230	225	I22-805	-9.27	0.01	-59.8	0.1	14.4
	D2.3	230	240	235	I22-808	-8.88	0.00	-56.8	0.2	14.2
	D2.4	240	250	245	I22-809	-8.92	0.01	-56.1	0.2	15.3
	D2.5	250	260	255	I22-810	-8.66	0.03	-55.2	0.6	14.1
	D2.6	260	270	265	I22-811	-8.89	0.03	-56.2	0.0	14.9
	D2.7	270	280	275	I22-812	-8.68	0.01	-54.6	0.1	14.8
	D2.8	280	290	285	I22-813	-8.45	0.00	-53.3	0.1	14.3
	D2.9	290	300	295	I22-814	-8.65	0.01	-55.1	0.0	14.1
	D3.0	300	310	305	I22-815	-9.03	0.03	-57.7	0.2	14.5
	D3.1	310	320	315	I22-816	-9.12	0.02	-58.9	0.1	14.1
	D3.2	320	330	325	I22-817	-8.79	0.00	-56.9	0.0	13.4
	D3.3	330	340	335	I22-818	-8.89	0.00	-57.4	0.6	13.7
	D3.4	340	350	345	I22-819	-8.49	0.02	-54.8	0.4	13.1
	D3.5	350	360	355	I22-820	-8.05	0.02	-51.7	0.4	12.7
	D3.6	360	370	365	I22-821	-8.37	0.02	-54.2	0.2	12.8
	D3.7	370	380	375	I22-822	-8.34	0.05	-53.2	0.1	13.5
	D3.8	380	390	385	I22-823	-8.73	0.03	-56.8	0.4	13.0
	D3.9	390	400	395	I22-824	-8.85	0.02	-57.1	0.2	13.7
	D4.0	400	410	405	I22-825	-8.43	0.01	-54.9	0.1	12.5
	D4.1	410	420	415	I22-826	-8.84	0.01	-58.6	0.5	12.1

	D4.2	420	430	425	I22-827	-9.25	0.03	-62.5	0.4	11.5
	D4.3	430	440	435	I22-828	-11.56	0.02	-79.7	0.4	12.8
R	R0.9	90	100	95	I22-829	-9.10	0.05	-59.8	0.3	13.0
SKUTA										
E	E0.0	0	10	5	I22-869	-5.92	0.05	-35.0	0.3	12.4
	E0.1	10	20	15	I22-870	-6.25	0.01	-38.3	0.1	11.7
	E0.2	20	30	25	I22-871	-6.78	0.03	-42.8	0.0	11.4
	E0.3	30	40	35	I22-872	-7.19	0.00	-45.6	0.6	11.9
	E0.4	40	50	45	I22-873	-7.27	0.01	-45.5	0.3	12.7
	E0.5	50	60	55	I22-874	-8.81	0.00	-57.2	0.0	13.3
	E0.6	60	70	65	I22-875	-10.32	0.00	-67.2	0.1	15.4
F	F0.0	0	10	5	I22-876	-6.13	0.04	-38.0	0.2	11.0
	F0.1	10	20	15	I22-877	-6.84	0.02	-42.7	0.3	12.0
	F0.2	20	30	25	I22-878	-6.51	0.00	-40.5	0.2	11.6
	F0.3	30	40	35	I22-879	-6.25	0.01	-38.2	0.2	11.8
	F0.4	40	50	45	I22-880	-6.31	0.03	-38.8	0.2	11.7
	F0.5	50	60	55	I22-881	-6.49	0.03	-40.5	0.2	11.4
	F0.6	60	70	65	I22-882	-7.02	0.01	-44.7	0.1	11.5
	F0.7	70	80	75	I22-883	-9.26	0.01	-61.4	0.2	12.7
	F0.8	80	90	85	I22-884	-9.14	0.04	-59.6	0.3	13.5
	F0.9	90	100	95	I22-885	-7.80	0.06	-50.5	0.3	11.9
	F1.0	100	110	105	I22-886	-7.74	0.06	-49.7	0.4	12.2
	F1.1	110	120	115	I22-887	-7.71	0.01	-50.2	0.4	11.5
	F1.2	120	130	125	I22-888	-7.66	0.00	-49.5	0.1	11.8
	F1.3	130	140	135	I22-889	-7.57	0.00	-48.8	0.2	11.8
	F1.4	140	150	145	I22-890	-7.47	0.02	-48.7	0.1	11.1
	F1.5	150	160	155	I22-891	-7.44	0.04	-47.5	0.0	12.0
	F1.6	160	170	165	I22-892	-7.47	0.04	-48.1	0.1	11.7
	F1.7	170	180	175	I22-893	-7.67	0.05	-48.4	0.1	13.0
	F1.8	180	190	185	I22-894	-7.66	0.02	-49.0	0.1	12.3
	F1.9	190	200	195	I22-895	-7.63	0.01	-48.6	0.2	12.4
	F2.0	200	210	205	I22-896	-7.68	0.04	-48.6	0.3	12.8
	F2.1	210	220	215	I22-897	-7.66	0.05	-48.5	0.2	12.8
	F2.2	220	230	225	I22-898	-7.69	0.04	-49.3	0.1	12.2
	F2.3	230	240	235	I22-899	-7.59	0.02	-48.7	0.1	12.0
	F2.4	240	250	245	I22-900	-7.58	0.05	-48.6	0.1	12.0
	F2.5	250	260	255	I22-901	-7.58	0.01	-48.5	0.0	12.1
	F2.6	260	270	265	I22-902	-7.56	0.01	-48.7	0.5	11.8
	F2.7	270	280	275	I22-903	-7.58	0.05	-48.1	0.4	12.5
	F2.8	280	290	285	I22-904	-7.60	0.03	-48.5	0.2	12.3
	F2.9	290	300	295	I22-905	-7.64	0.00	-48.9	0.5	12.2
	F3.0	300	310	305	I22-906	-7.58	0.02	-48.6	0.2	12.0
	F3.1	310	320	315	I22-907	-7.66	0.04	-48.7	0.0	12.6
	F3.2	320	330	325	I22-908	-7.75	0.01	-48.9	0.2	13.1
	F3.3	330	340	335	I22-909	-8.44	0.04	-53.4	0.3	14.1
	F3.4	340	350	345	I22-910	-8.21	0.03	-52.4	0.1	13.3

	F3.5	350	360	355	I22-911	-8.95	0.02	-56.3	0.0	15.3
	F3.6	360	370	365	I22-912	-8.90	0.00	-54.2	0.4	17.0
	F3.7	370	380	375	I22-913	-9.04	0.03	-54.9	0.6	17.4
	F3.8	380	390	385	I22-914	-9.17	0.02	-55.4	0.0	18.0
	F3.9	390	400	395	I22-915	-9.13	0.00	-55.8	0.6	17.2
	F4.0	400	410	405	I22-916	-9.02	0.06	-55.1	0.1	17.1
	F4.1	410	420	415	I22-917	-8.91	0.00	-54.3	0.2	17.0
	F4.2	420	430	425	I22-918	-8.92	0.04	-54.6	0.1	16.8
	F4.3	430	440	435	I22-919	-8.82	0.01	-54.4	0.3	16.2
	F4.4	440	450	445	I22-920	-8.81	0.03	-54.6	0.3	15.9
	F4.5	450	460	455	I22-921	-8.84	0.04	-54.6	0.9	16.1
	F4.6	460	470	465	I22-922	-8.76	0.01	-53.8	0.6	16.3
	F4.7	470	480	475	I22-923	-8.66	0.01	-54.1	0.6	15.2
	F4.8	480	490	485	I22-924	-8.76	0.01	-54.5	0.2	15.6
	F4.9	490	500	495	I22-925	-8.64	0.04	-54.3	0.0	14.8
	F5.0	500	510	505	I22-926	-8.53	0.00	-53.1	0.1	15.1
	F5.1	510	520	515	I22-927	-8.62	0.04	-53.9	0.3	15.1
	F5.2	520	530	525	I22-928	-8.68	0.02	-53.9	0.4	15.5
	F5.3	530	540	535	I22-929	-8.63	0.00	-53.8	0.2	15.2
	F5.4	540	550	545	I22-930	-8.63	0.02	-53.6	0.1	15.4
	F5.5	550	560	555	I22-931	-8.70	0.04	-54.0	0.3	15.6
	F5.6	560	570	565	I22-932	-8.75	0.02	-54.8	0.4	15.2
	F5.7	570	580	575	I22-933	-8.75	0.01	-54.7	0.2	15.3
	F5.8	580	590	585	I22-934	-8.71	0.00	-55.2	0.2	14.5
	F5.9	590	600	595	I22-935	-8.71	0.02	-54.8	0.5	14.9
	F6.0	600	610	605	I22-936	-8.85	0.01	-55.6	0.1	15.2
	F6.1	610	620	615	I22-937	-9.11	0.01	-58.0	0.4	14.9
	F6.2	620	630	625	I22-938	-9.06	0.03	-57.7	0.2	14.8
	F6.3	630	640	635	I22-939	-9.00	0.01	-58.3	0.6	13.7
	F6.4	640	650	645	I22-940	-8.65	0.01	-55.3	0.3	13.9

Table S3. ^{3}H results for Triglav Glacier and Skuta Glacier.

Sample	Combined ice core sections	Depth (cm)			^{3}H (TU)	±1σ (TU)
		from	to	mid		
TRIGLAV GLACIER						
TRIG-1	AT-BT	-10	0	-5	5.86	0.08
TRIG-2	A0.0, B0.0, A0.1, B0.1, A0.2, B0.2	0	30	15	6.49	0.07
TRIG-3	A0.3, B0.3, A0.4, B0.4, A0.5, B0.5	30	60	45	6.30	0.07
TRIG-4	A0.6, B0.6, A0.7, B0.7, A0.8, B0.8, R0.9	60	100	80	5.48	0.07
TRIG-5	C1.0, C1.1, C1.2, C1.3, D1.3, C1.4, D1.4, C1.5, D1.5	100	160	130	0.07	0.02
TRIG-6	C1.6, D1.6, C1.7, D1.7, C1.8, D1.8, C1.9, D1.9	160	200	180	0.12	0.02
TRIG-7	C2.0, C2.1, D2.1, D2.0A, D2.0B, C2.2, C2.3, D2.3	200	240	220	0.15	0.02
TRIG-8	C2.4, D2.4, C2.5, D2.5, C2.6, D2.6	240	270	255	0.07	0.02
TRIG-9	C2.7, D2.7, C2.8, D2.8, C2.9, D2.9	270	310	290	0.11	0.02
TRIG-10	C3.1, D3.1, C3.2, D3.2, C3.3, D3.3	310	340	325	0.06	0.02

TRIG-11	C3.4, D3.4, C3.5, D3.5	340	360	350	0.05	0.03
TRIG-12	C3.6, D3.6, C3.7, D3.7	360	380	370	0.14	0.02
TRIG-13	D3.8, D3.9	380	400	390	0.09	0.03
TRIG-14	D4.0, D4.1	400	420	410	0.09	0.03
TRIG-15	D4.2, D4.3	420	440	430	0.06	0.03
SKUTA GLACIER						
Skuta-1	F0.0-F0.3	0	40	20	6.94	0.15
Skuta-2	F0.4-F0.7	40	80	60	6.41	0.11
Skuta-3	F0.8-F1.1	80	120	100	3.38	0.08
Skuta-4	F1.2-F1.5	120	160	140	2.97	0.07
Skuta-5	F1.6-F1.9	160	200	180	3.17	0.07
Skuta-6	F2.0-F2.3	200	240	220	2.97	0.06
Skuta-7	F2.4-F2.7	240	280	260	3.34	0.07
Skuta-8	F2.8-F3.1	280	320	300	/	/
Skuta-9	F3.2-F3.5	320	360	340	3.33	0.07
Skuta-10	F3.6-F3.9	360	400	380	2.48	0.06
Skuta-11	F4.0-F4.3	400	440	420	/	/
Skuta-12	F4.4-F4.7	440	480	460	2.64	0.06
Skuta-13	F4.8-F5.1	480	520	500	/	/
Skuta-14	F5.2-F5.5	520	560	540	2.64	0.06
Skuta-15	F5.6-F5.9	560	600	580	/	/
Skuta-16	F6.0-F6.4	600	645	622.5	2.79	0.06

	Skuta-5	160 to 200	<0.08	<0.011	0.12±0.02
	Skuta-6	200 to 240	<0.08	<0.008	0.21±0.02
	Skuta-7	240 to 280	<0.08	<0.007	0.35±0.02
	Skuta-8	280 to 320	<0.08	<0.005	0.13±0.01
	Skuta-9	320 to 360	<0.08	<0.008	0.16±0.02

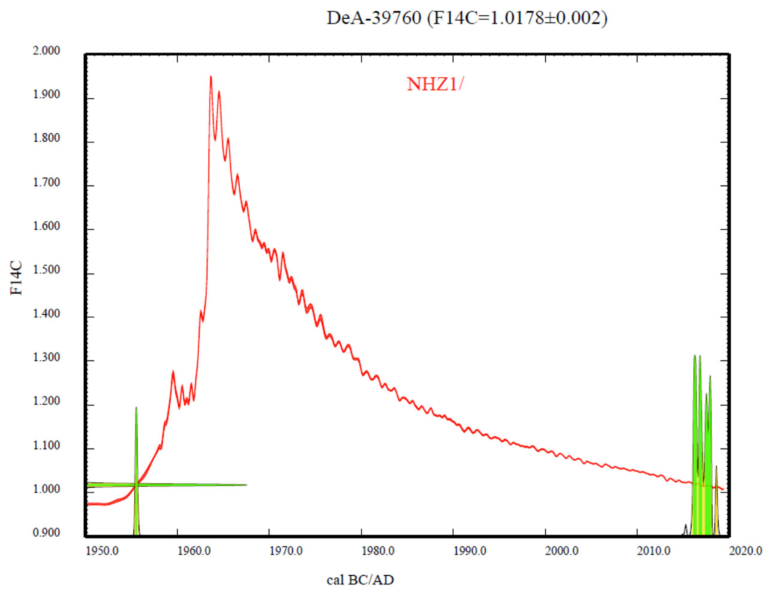

Figure S4. Radiocarbon age calibration plot for sample DeA-39760

Table S4. Obtained calibrated ages (cal AD) for the stem plant sample from Triglav Glacier based on measured $F^{14}C$ of 1.0178±0.002 (sample DeA-39760).

68% confidence	Mean	95% confidence	Mean
1955.46 to 1955.61	1955.61	1955.35 to 1955.75	1955.55
2016.11 to 2016.48	2016.48	2015.98 to 2018.14	2017.06
2016.71 to 2017.05	2017.05	2018.51 to 2018.76	2018.64
2017.40 to 2018.06	2017.73		

Table S5. ^{7}Be, ^{137}Cs and ^{210}Pb activity (Bq/kg) in ice from Triglav Glacier and Skuta Glacier.

Glacier	Sample	Depth (cm)	^{7}Be	^{137}Cs	^{210}Pb
Triglav	TRIG-1	-10 to 0	5.73±0.13	0.264±0.008	23.91±0.72
	TRIG-2	0 to 30	0.96±0.07	0.053±0.007	4.19±0.17
	TRIG-3	30 to 60	<0.08	<0.038	0.31±0.06
	TRIG-4	60 to 100	<0.08	0.016±0.003	0.92±0.05
	TRIG-5	100 to 160	<0.08	<0.066	0.56±0.10
	TRIG-6	160 to 200	<0.08	<0.008	0.11±0.02
	TRIG-7	200 to 240	<0.08	<0.047	<0.34
	TRIG-8	240 to 270	<0.08	<0.033	<0.24
	TRIG-9	270 to 310	<0.08	<0.054	<0.39
	TRIG-10	310 to 340	<0.08	<0.045	<0.31
	TRIG-11	340 to 360	<0.08	<0.055	<0.36
Skuta	Skuta-1	0 to 40	0.74±0.06	0.094±0.008	4.69±0.17
	Skuta-2	40 to 80	0.18±0.02	0.013±0.003	0.71±0.04
	Skuta-3	80 to 120	<0.08	<0.007	0.09±0.01
	Skuta-4	120 to 160	<0.08	<0.006	0.09±0.02

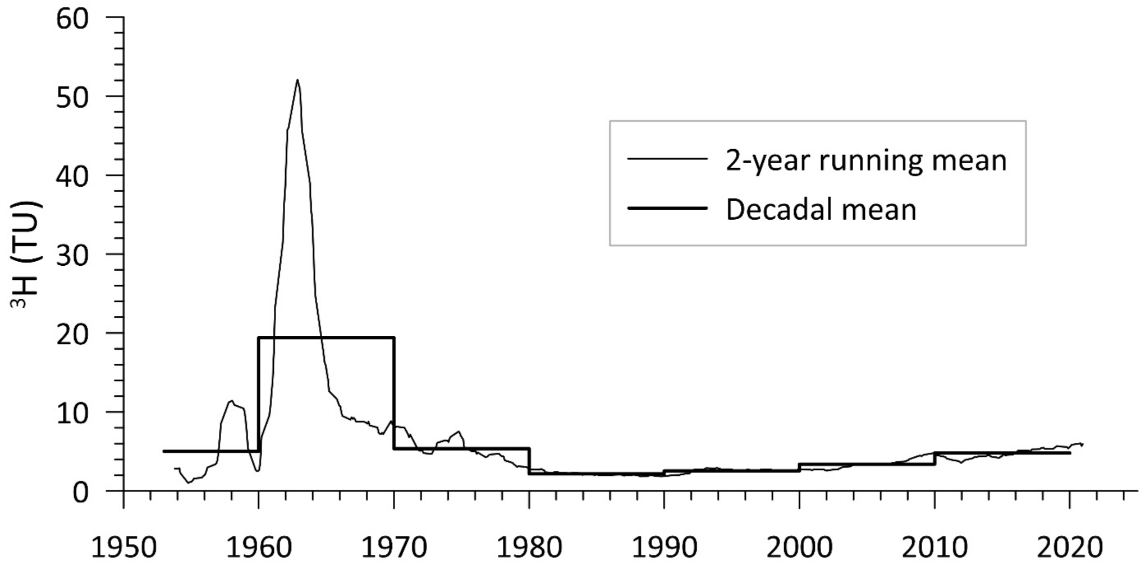

Figure S5. Winter period tritium concentrations of Vienna precipitation (2-year running mean and decadal mean), decay corrected to the sampling year of 2022.

Age-depth modelling by tuning of the δ^{18}O time-series to lake Jezero v Ledvicah reconstructed temperature record (Battarbee et al., 2002)

Table S6. Tie-points for the construction of the age-depth model for the Triglav Glacier and Skuta Glacier δ^{18}O records

Triglav depth (cm)	Skuta depth (cm)	Jezero v Ledvicah record (year)
95	85	1955.55
205	385	1902.36
355	595	1862.36

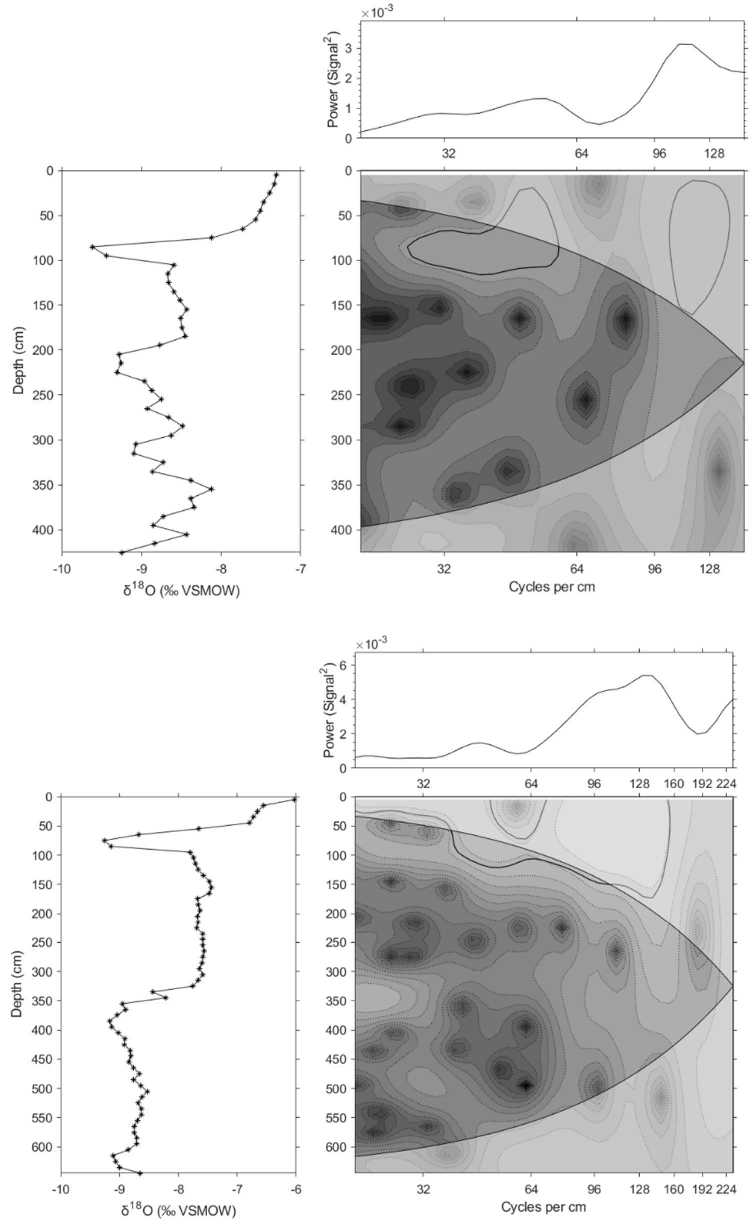

Figure S6. Spectral comparison of the Triglav (top) and Skuta (bottom) δ^{18}O records as a function of depth (cm). Both δ^{18}O profiles indicate similar δ^{18}O vertical profile, though smoothed for Skuta. The local wavelet spectrum (bottom-right panel) marks the most intense periodicities (brightern shade) at specific depth bands. Black contour lines indicate significant coherence. Conversely, the global wavelet power spectrum (top panel) indicates the frequencies with stronger presence across all depths in the ice cores. The significance level is p=0.05 within the cone of influence in all cases. In general, the figure shows that the Triglav and Skuta δ^{18}O records have a distinctive local power spectrum at specific depths, owing to their different location and intrinsic accumulation and compaction rates but an overall similar global spectrum. Both records present a lower and significant period (<64 cycles) at the first 100 cm. Nevertheless, the dominant period lies above the 64 cycles determined by the light shade in the wavelet and the peak in the power spectrum (i.e., 96-128 cycles) graphs. This global coherence in the Triglav and Skuta δ^{18}O spectral signal suggests a global dominant climatic control (>64 cycles) ultimately dependent and tuned by local depositional processes at specific depths and frequencies (<64 cycles).